X-RAY DIFFRACTION OF MYELIN MEMBRANE

I. Optimal Conditions for Obtaining Unmodified Small Angle Diffraction Data from Frog Sciatic Nerve

C. K. AKERS *and* D. F. PARSONS

From the Biophysics Department, Roswell Park Memorial Institute, Buffalo, New York 14203

ABSTRACT The X-ray diffraction pattern of myelin of frog sciatic nerve has been investigated, using a Kratky small angle slit camera to obtain the electron density distribution across the membrane. All major reflections observed were related to a fundamental repeat distance of 171 ± 2.8 A. There was no further increase in the number of reflections on varying the experimental conditions (varying pH, applying tension, immersion in various isotonic buffer solutions, etc.) or by varying the camera slit arrangement. The degree of disorder within the myelin sheath was examined by comparing the crystallite size to the half-width of the diffraction peak at half-height. The limiting of the diffraction spectra to five major reflections was determined not to be caused by disorder. It is concluded that the observed X-ray diffraction pattern is a consequence of the particular electron density distribution of the membrane. Therefore, the membrane cannot contain sharply distinct step-function regions of electron density, but approaches a modified cosine distribution.

INTRODUCTION

Myelin remains the only example of a cell membrane giving sufficiently detailed X-ray diffraction spectra, (Schmitt, Bear, and Clark, 1935; Finean, 1953; Fernandez-Moran and Finean, 1957; Finean, 1958; Blaurock and Worthington, 1969) in the natural state, to allow the electron density distribution across the membrane to be calculated (Finean, 1962; Finean and Burge, 1963; Burge and Draper, 1965; Worthington and Blaurock, 1968). Attempts to pack other membranes (Finean, Sjostrand, and Steinmann, 1953; Finean, 1965; Finean, Coleman, Green, and Limbrick, 1966 *a*; Finean, Coleman, and Green, 1966 *b*; Worthington, 1960; Husson and Luzzati, 1963; Blasie, Dewey, Blaurock, and Worthington, 1965; Robertson, 1966; Silvester, 1964; Burge and Draper, 1967) in an ordered array have met with only limited success, the reflections being both weaker and fewer in number than those of myelin. Hence, in spite of the atypical character of myelin in relation to the composition (Norton and Autilio, 1965) and function (O'Brien, 1967) of other membranes,

myelin represents an important case for cell membrane structure analysis. Five principal sharp reflections and three higher order weak reflections can be obtained on X-ray diffraction of whole nerve. If these could be phased correctly, the electron density distribution across the membrane could be calculated with some precision and the packing arrangement of protein and lipid could be better defined. Extensive past work on X-ray diffraction of myelin (Finean, 1962; Finean and Burge, 1963; Burge and Draper, 1965; Worthington and Blaurock, 1968) was interpreted to give good support for the lipid bilayer model for myelin.

A primary point requiring investigation in a reexamination of the problem of the myelin structure is whether the limited number of reflections (five of significant intensity) is a consequence of disorder in the myelin membrane arrays, a deficient X-ray technique, or whether it is a consequence of the electron density distribution of the membrane. The present work also provides a new method of phasing reflections which does not depend on swelling of myelin and possible disorganization of the membranes as a result of swelling.

In this report (part I), we have investigated how the number of reflections and their relative intensities are affected by the specimen conditions and the camera arrangement. In the following paper (part II) we have used a new approach (heavy metal labeling) to determine the phases of the reflections. The appropriate transform relating structure amplitude to electron density has been reconsidered, and finally, the electron density distribution of the myelin membrane has been recalculated.

MATERIALS AND METHODS

Grass frogs (*Rana pipiens*) were pithed and the sciatic nerve removed. The nerve was placed under slight tension by hanging a 10 g weight on each end. While under tension, the nerve was immersed in phosphate buffered saline (PBS) (Dulbecco and Vogt, 1954) and sealed in an aluminum chamber (Fig. 1) having Mylar windows 0.5 thousandths of an inch thick. The chamber could be maintained within 4–7°C for periods of more than 6 hr by a solid CO_2 cooling unit fitted with a heat-valve device. The nerve was placed parallel to the slits of the camera. The X-ray generator was a Siemens Crystalloflex IV (Siemens America, Inc., New York, N.Y.). The Kratky X-ray tube (Siemens America, Inc.), operated at 30 kv and

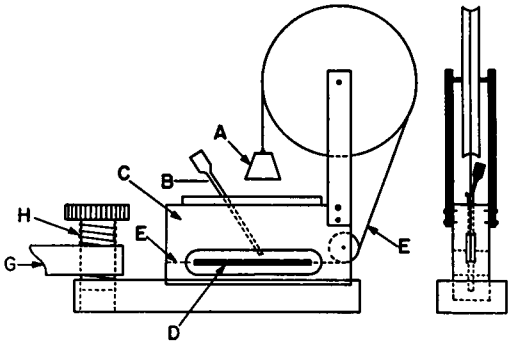

FIGURE 1 Sample holder for holding sciatic nerve under tension while immersed in PBS (front and side view). *A*, weight; *B*, entrance for buffer solution; *C*, cell chamber wall; *D*, nerve in cell; *E*, string that connects the weight to the nerve; *G*, arm of heat valve connected to a rod immersed in dry ice in a Dewer flask; *H*, heat valve.

TABLE I

EXPERIMENTAL SLIT ARRANGEMENTS ON THE KRATKY CAMERA

Arrangement	Entrance slit	Exit slit	Step size Δ 2 θ		Minimum counts detected (n)	% standard deviation ($1/\sqrt{n}$)	Time
	μ	μ	*milliradians*	*mm*			*min*
a	121	200	0.95	0.20	1000	3.16	1
b	121	100	0.47	0.10	1000	3.16	1
c	80	80	0.38	0.08	1000	3.16	2
d	40	40	0.19	0.04	400	5.00	4
e	121	100	0.95 2.35	0.20 0.50	3000	1.82	4

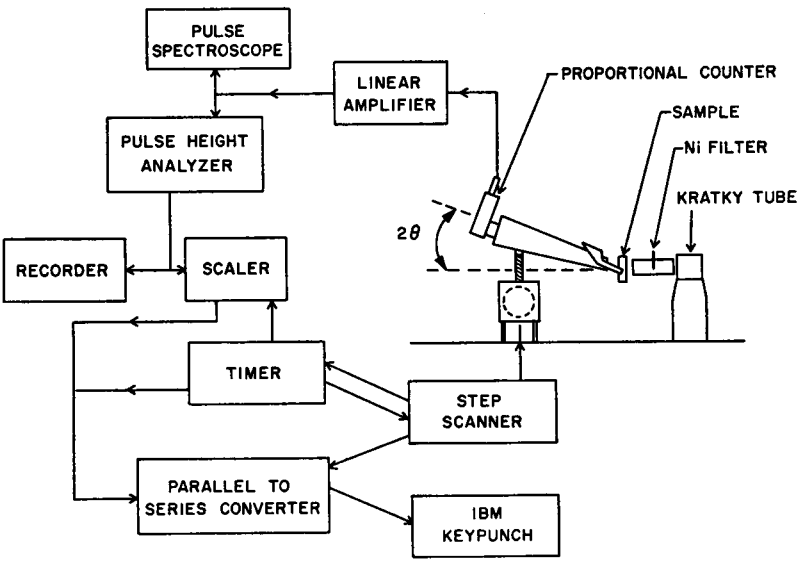

FIGURE 2 Block diagram of automated small angle X-ray scattering apparatus.

30 mamp had a copper anode having a line focus of 7 mm by 0.25 mm. The line focus was viewed at a take-off angle of 5°. The X-rays were filtered with a nickel filter, 0.0004 of an inch thick. Additional monochromatization of the X-rays was obtained by the use of a single channel pulse height analyzer (Siemens America, Inc.) centered on the CuKα radiation. This was continuously monitored with a pulse spectroscope (Siemens America, Inc.). The X-rays were collimated using a Kratky collimation system (Kratky, 1963). Various entrance slits were used in this investigation. A list of the various instrumental conditions with the entrance slits is given in Table I.

The diffraction pattern was measured with a proportional detector (Siemens America, Inc., type B) operated at 1900–1950 v DC. The proportional counter was 306.96 mm from the sample. The space between the detector and sample, and also the collimator block, was

evacuated to 10^{-2} mm of mercury. The diffraction pattern was scanned automatically by means of a step motor drive for the proportional counter scanning mechanism (Fig. 2). The step motor was controlled by a Step Scanner Programmer (Humphrey Electronics, Inc., Raleigh, N.C.) which enabled the angle increments to be preprogrammed. A Parallel-to-Series Converter Unit (Humphrey Electronics, Inc.) passed the data (counts, counting time and camera angle setting) to an IBM 526 Key Punch.

The angular calibration of the camera was based on a precision measurement of the distance from the center of the sample holder along a line joining the center of the detector to a point overlying the center of the detector elevating screw (Fig. 3) which is 210.87 mm. The detector elevating screw was calibrated in millimeters, and could be read by a vernier to less than 10 μ. The beam center (m_0, mm on the screw) was found by narrowing down the exit slit and insertion of a 5 mm aluminum filter. The scattering angle (2θ) at any other setting (m, mm on the elevated screw) was obtained from

$$\sin(2\theta) = (m - m_0)/210.87. \quad (1)$$

Integrated intensities were obtained measuring the area under each peak above the base line by weighing paper. The percentage error in weighing the (400) peak was 10%. Beam divergence was measured by exposing X-ray film at the position of the sample and at the position of the detector.

Electron microscopy of thin sections was used to check that the frog sciatic nerve showed no structural abnormalities. Pieces of nerve adjacent to that used for X-ray diffraction were fixed for 1-½ hr in Palade's buffered osmium tetroxide solution (Palade, 1952). Some sciatic nerves were prefixed for 4 hr in 4% paraformaldehyde in PBS (produced by dissociation of 4% paraformaldehyde solution) before fixation with Palade's osmium tetroxide solution for 1-½ hr. Specimens were then dehydrated with acetone and embedded in Epon (Shell Chemica

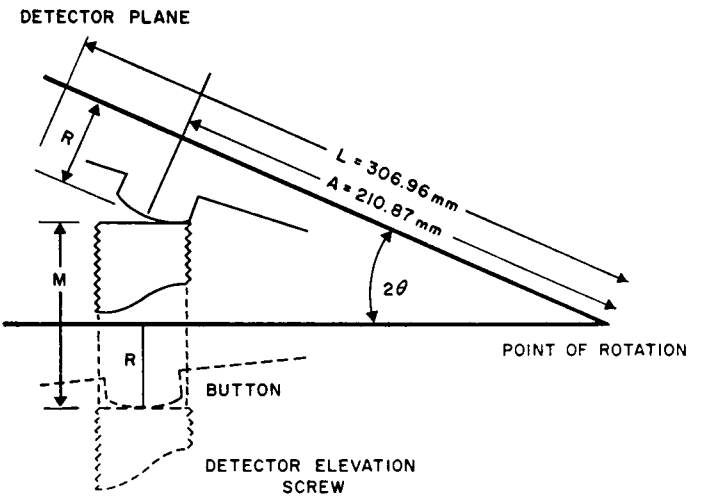

FIGURE 3 Scanning mechanism of step motor in determining two theta position of proportional counter. R = distance of X-ray camera midplane to bottom of spherical button; M = distance step motor has elevated the proportional counter; A = distance between pivot point and button center; L = distance between pivot point and the detector plane. (sin [2θ] = M/A)

Co., New York, N.Y.) (Luft, 1961). Blocks were polymerized for 16 hr at 70°C and sectioned with an LKB (Laboratorie och Kemikaliska Produkter, Stockholm, Sweden) ultramicrotome using a diamond knife (Instituto Venezolano de Investigaciones Cientificas—I.V.I.C. Carácas, Venezuela). Sections were stained with basic lead citrate (Venable and Coggeshall, 1965). Thick unstained Epon sections were also examined by phase contrast light microscopy. Some sciatic nerves were fixed for 2 hr in a phosphate buffered solution containing 4% of pure formaldehyde (pH 7.2) produced by dissociation of a 4% solution of paraformaldehyde, (Pease, 1964) and processed and sectioned for light microscopy using hemotoxylin and eosin staining.

RESULTS

Circular Beam Diffraction Pattern

Circular cross-section beam diffraction patterns were taken on a modified Siemens flat camera. The collimation was achieved with two electron microscope apertures (one 100 μ and one 200 μ hole size) spaced 38 mm apart. The collimator was 5 mm from the sample, and the sample to film (Kodak No-screen Medical X-ray [Eastman Kodak Co., Rochester, N.Y.]) distance was 215 mm. Exposure time was either 2.5 hr for preliminary experiments or 16 hr for data collection. The patterns showed a fiber-like pattern which has been reported earlier (Schmitt et al, 1935). The pattern had a half-angle spread of approximately 15°. The spread of the half angle was independent on the amount of tension applied to the nerve from 0–40 g. The intensity pattern showed an alternating pattern similar to the slit collimating diffraction pattern. No further small-angle reflections were seen in the photographs under these camera conditions other than the five major reflections. However, this is being further investigated using a high intensity microfocus X-ray camera. The wide angle region was also examined and will be discussed in a later paper.

Rectangular Beam Pattern

A typical small angle X-ray diffraction pattern is shown in Fig. 4 *A*. The lipid-extracted curve (cell filled with PBS) is shown in Fig. 4 *B*. The beam profile is shown in Fig. 4 *C* showing that the region of interest is away from the scattering of the beam profile. The diffraction pattern of the first five orders of a 171 A spacing agrees with the previous reported work (Schmitt et al, 1935; Finean, 1953; Fernandez-Moran and Finean, 1957; Finean and Burge, 1963; Moody, 1963; Worthington and Blaurock, 1968). Various minor peaks that are not orders of the 171 A repeat could not be detected using film technique and have not been reported before.

The spacing of the first five principal reflections ($h00$), excluding weak and non-reproducible higher order reflections, are given in Table II. The intensity of the 6th, 8th, and 11th order reflections were very weak (Table III). Therefore, these reflections could only cause small changes in the electron density distribution given by the five major reflections. The reflections agree with the expected values for successive orders of a fundamental of 171 $\pm$ 2.8 A. In addition to the principal reflections, we

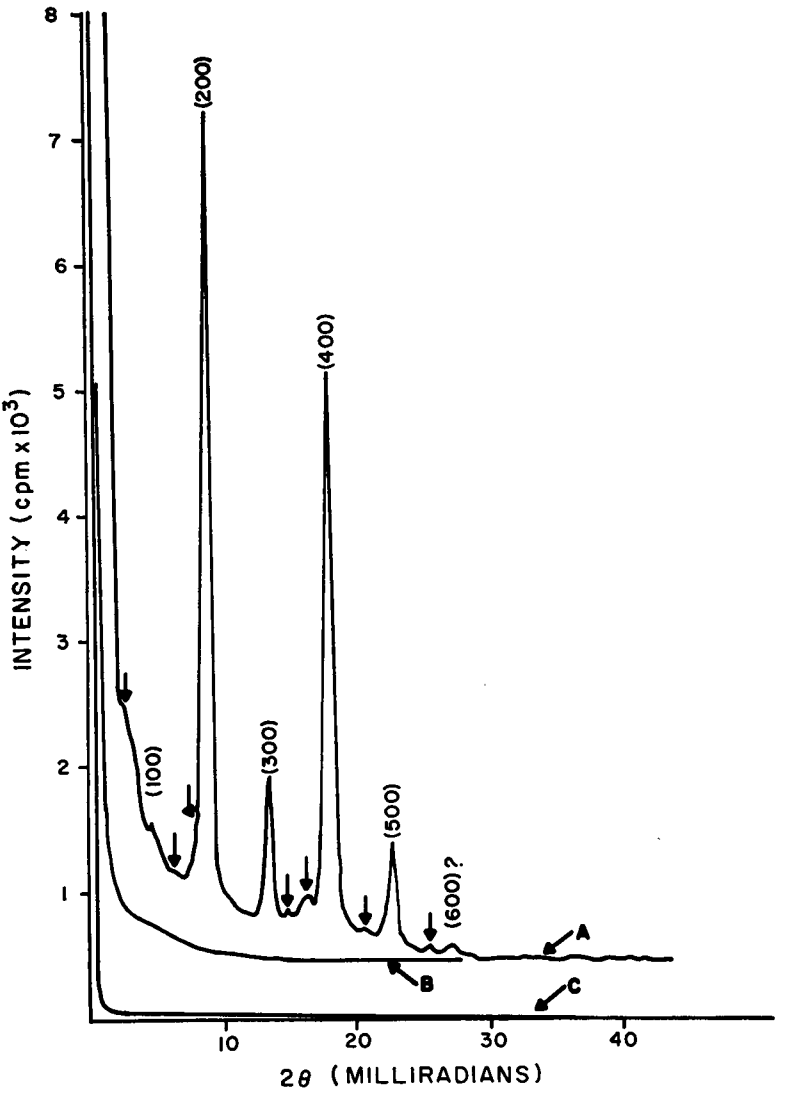

FIGURE 4 Typical small angle diffraction diagram obtained with the Kratky slit camera showing equatorial reflections from frog sciatic nerve. *A*, complete pattern of untreated nerve; nonprincipal reflections are shown by the pointers; principal reflections are labeled. *B*, diffraction pattern showing the curve produced by a lipid-extracted nerve. *C*, beam profile.

observed other low intensity, but significant equatorial peaks (Fig. 4 *A*). These peaks may give more information on the structure of the double myelin membrane repeat unit, and are being investigated further. It was noticed that not all of the anomalous peaks appeared in every diffraction pattern. However, they appeared sufficiently often to be considered significant.

TABLE II

PRINCIPAL SMALL ORDER SPACINGS IN MYELIN DIFFRACTION PATTERN

	(100)	(200)	(300)	(400)	(500)
XM 134	175 (168.6)*	84.3	56.0 (56.2)	41.9 (42.1)	33.6 (33.9)
XM 135	175 (168.6)	84.3	56.0 (56.2)	42.1 (42.1)	33.4 (33.9)
XM 136	175 (165.6)	82.8	55.5 (55.2)	41.1 (41.4)	32.8 (33.1)
XM 143	171 (167.4)	83.7	56.5 (55.8)	41.6 (41.8)	33.1 (33.5)
XM 139–1	170 (172.2)	86.6	56.9 (57.7)	42.7 (43.8)	34.0 (34.6)
XM 139–2	170 (168.6)	84.3	55.5 (56.2)	41.9 (42.1)	33.1 (33.7)
XM 145	171 (166.6)	83.3	55.0 (55.5)	41.6 (41.6)	33.4 (33.3)
XM 148	170 (168.6)	84.3	56.0 (56.2)	42.1 (42.1)	33.8 (33.9)
XM 149	166 (166.6)	83.3	55.9 (55.5)	41.9 (41.6)	33.6 (33.3)
XM 157	174 (172.2)	86.6	57.5 (57.7)	43.0 (43.8)	34.5 (34.6)
XM 140	170 (168.6)	84.3	56.0 (56.2)	41.9 (42.1)	33.6 (33.7)
XM 153	176 (172.2)	86.6	58.5 (57.7)	42.7 (43.3)	34.1 (34.6)
XM 151	172 (172.2)	86.6	56.4 (57.7)	42.7 (43.3)	34.3 (34.8)
XM 156	170 (172.2)	86.6	58.0 (57.7)	44.1 (43.3)	34.7 (34.6)
XM 158	166 (172.2)	86.6	57.4 (57.7)	41.9 (43.3)	33.4 (34.6)
XM 154	172 (175.4)	87.7	58.0 (58.5)	43.3 (43.8)	34.5 (34.6)
Mean (observed)	171.4	85.1	56.5	42.2	33.7
Standard error	2.8	1.5	1.0	0.7	0.5
%	1.76	1.76	1.75	1.65	1.48

* Spacing in parenthesis is based on fundamental that was calculated from the (200).

The individual peak and integrated intensities varied in different experiments due to small differences in thickness of the frog sciatic nerve and in the alignment of each nerve. In this report we have measured the integrated intensities (area under peak) rather than peak values. The results for the five major reflections (Table II) are tabulated with reference to the tension applied to the nerve during diffraction in Table IV. The sciatic nerve showed a large initial elongation of 10% on applying 4 g weight tension, indicating some initial wrinkling of the unstretched nerve. However, removal of this wrinkling did not reduce the arcing of circular beam patterns. Thus, the various weights that were used to stretch the nerve did not straighten the tubes of myelin membranes. The elasticity of the myelin sheath might be restricted by collagen fibers within the nerve. The degree of undulation of the myelin sheath in the unstretched nerve was also examined by phase contrast light microscopy of thick Epon-embedded electron microscope transverse and longitudinal sections (Figs. 5 *A* and 5 *B*). Epon sections indicated some small scale irregularity. Tension applied to the nerves from 4–40 g showed a reversible elastic elongation of 0.45% per g. The intensities showed no definite relation to tension. A value of 10–20 g weight was used in all subsequent experiments, and results for all tensions were averaged together.

TABLE III

INTENSITY AND SPACING OF MINOR LARGE ORDER REFLECTIONS

	(600)		(800)		(1100)	
	Intensity*	Spacing	Intensity	Spacing	Intensity	Spacing
		A		*A*		*A*
XM 558	0.9	28.7	0.9	21.5	1.0	15.4
XM 560	0.5	28.5	1.2	21.4	0.9	15.4
XM 561	0.6	28.5	0.8	21.2	1.1	15.3
XM 562	0.5	28.5	0.5	21.4	1.2	15.4
XM 563	0.3	28.6	0.6	21.3	1.4	15.4
Average	0.76 ± .26	28.6	0.8 ± .20	21.4	1.1 ± 0.16	15.4
Calculated		28.5		21.4		15.5

* Intensity based on (200); see Table IV.

TABLE IV

INTENSITIES OF GRASS FROG SCIATIC NERVE USING VARIED WEIGHTS IN STRETCHING CELL*

	(100)	(200)‡	(300)	(400)	(500)	Weight
XM 134	NOBS*	100	17.7	44.5	9.5	0
XM 135	1.2	100	15.7	48.2	10.3	0
XM 136	1.3	100	19.7	60.8	12.6	0
XM 143	0.9	100	14.3	55.4	11.1	10
XM 139–1	1.0	100	8.4	59.1	10.8	10
XM 139–2	0.5	100	16.9	64.6	13.4	10
XM 145	1.6	100	17.3	61.4	15.3	10
XM 140	0.8	100	14.3	46.0	11.0	20
XM 148	0.6	100	13.6	51.6	10.1	20
XM 149	1.8	100	15.1	48.9	12.7	20
XM [illegible]	1.0	100	15.1	51.3	11.9	20
XM 153	1.3	100	11.7	55.4	9.8	30
XM 151	0.9	100	11.9	52.0	10.6	30
XM 156	NOBS	100	12.3	59.9	7.2	30
XM 158	0.9	100	13.8	45.8	11.3	30
XM 154	0.6	100	8.1	58.7	7.2	40
Mean (observed)	0.90	—	13.61	54.1	10.9	
Standard error	0.37	—	2.93	5.8	2.08	
%	41.	—	21.5	10.8	19.0	

* Experimental arrangement *b*, immersed in PBS, pH 7.2, 4–7°C.

‡ (200) used as reference.

§ NOBS—Nonobserved reflection.

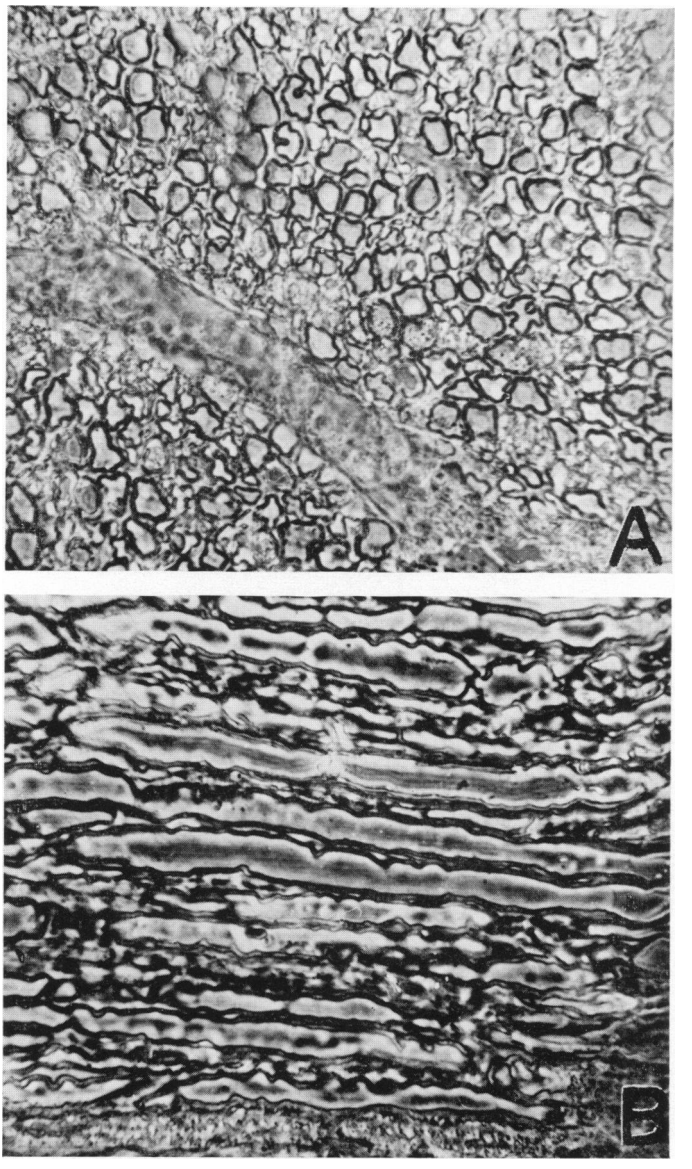

FIGURE 5 Phase contrast light microscopy of thick Epon-embedded, osmium-tetroxide-fixed, sciatic nerve. *A*, transverse section; the myelin layers are distorted cylinders and show irregular transverse packing arrangement (magnification, 1360× plate 589); some of the distortion may be due to the fixation and embedding process. *B*, longitudinal section; the section is cut slightly obliquely; the myelinated axons follow fairly straight paths along the nerve axis (magnification 680×, plate 590).

The degree of reproducibility of the integrated intensities was mainly related to the total number of counts per reflection. With respect to the (400) peak, the observed standard deviation represented 10.8% of the mean. The error in the measurement of the area under the (400) peak was 12.7%. Factors affecting the reproducibility will be discussed further (Discussion). We obtained no electron microscope evidence of significant structural differences between different preparations. The transverse thin sections of the sciatic nerve (Fig. 6) showed regular arrays of membrane pairs.

The effects of temperature, pH, osmolarity, and ionic composition on the diffraction pattern were investigated in order to determine the effects of deviations from physiological conditions on relative integrated intensities. No difference was found for the diffraction pattern obtained at room temperature compared to that taken at 4 C. (We will discuss wide angle reflections in a separate report). Deviation in pH of ± 0.4 away from 7.2 and in osmolarity had a large effect on relative intensities. No difference was found, either in X-ray diffraction or electron microscopy, between

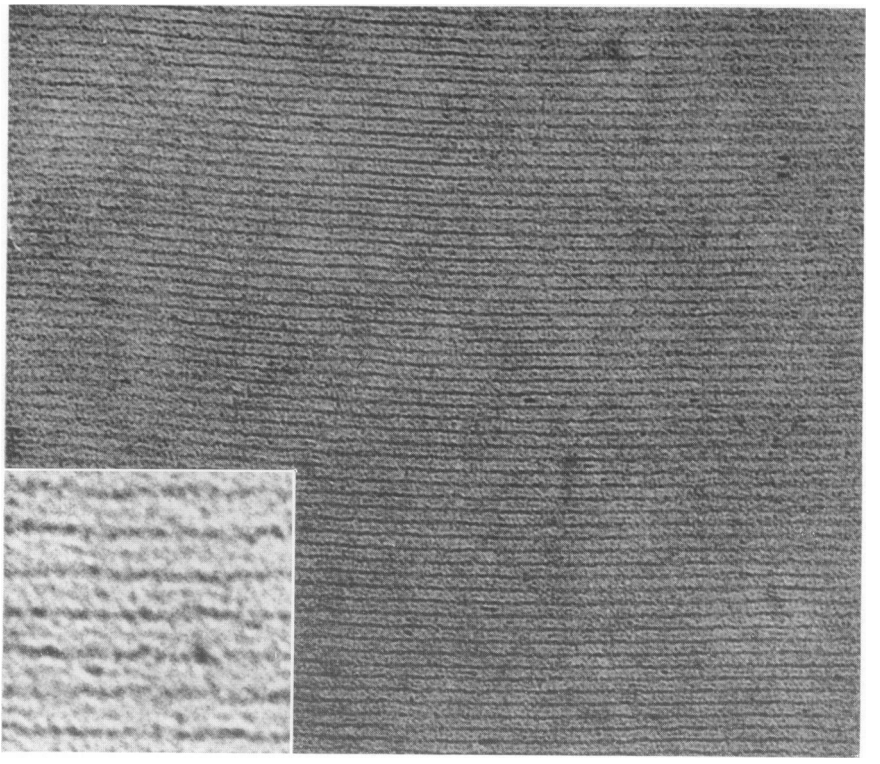

FIGURE 6 Thin section of sciatic nerve that was fixed 4 hr in 4% formaldehyde followed by 1-1½ hr in Palade's osmium tetroxide. The myelin tubes are made up of about 75 layers of myelin membrane pairs. The layering appears very regular in nearly all parts of the nerve. The dense line is the cytoplasmic surface of the membrane, and the lightly stained intraperiod line is the external surface of the membrane; (magnification 100,000×; insert magnification 320,000×, plate 829).

various isotonic solutions, PBS (Dulbecco and Vogt, 1954), Ringer's solutions (NaCl, 6.0 g; KCl, 0.14 g; $NaHCO_3$, 0.5 g; $CaCl_2$, 0.24 g; in 1000 ml, adjusted to pH 7.2 with CO_2), and normal saline.

Nerves were also examined by electron microscopy at the end of the diffraction experiments (2 hr immersion in PBS at 4°C). No significant changes were seen.

To determine if we were recording the diffraction pattern of a completely hydrated nerve, we allowed a nerve to dehydrate slowly in the diffraction cell and recorded X-ray diffraction patterns over a period of 16 hr. A significant degree of dehydration caused a change in the intensity distribution as well as a change in the fundamental spacing (Fig. 7). Only X-ray diffraction patterns that represented fully-hydrated myelin membranes were used in this study.

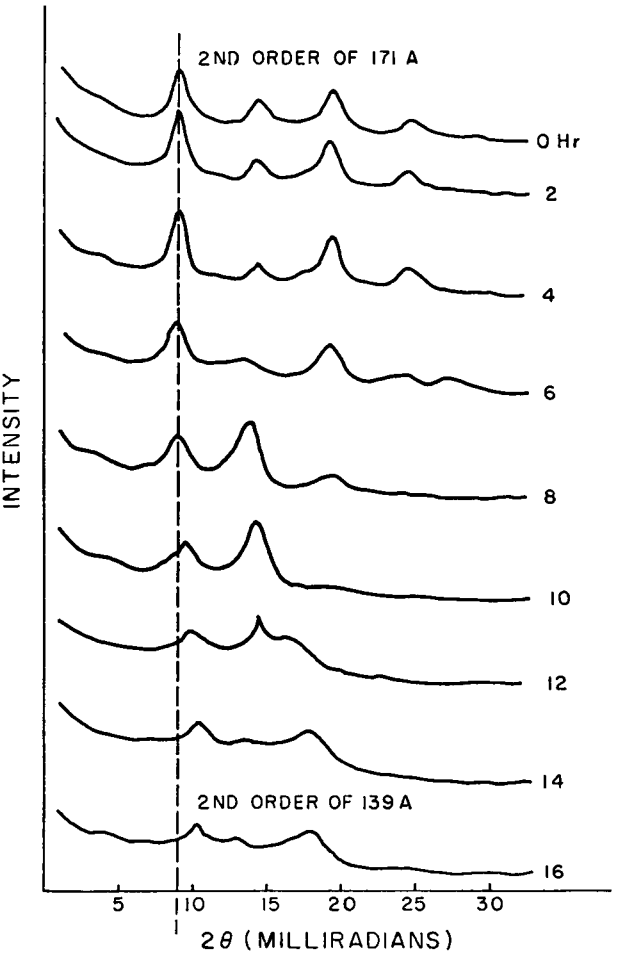

FIGURE 7 Effect of slow drying (over 16 hr) of frog sciatic nerve to show changes in fundamental spacing and the intensity distribution.

Intensity Corrections

We examined each of the possible intensity corrections to determine if they were to be applied to the observed intensities of the myelin diffraction data. If the effect was less than the experimental error, then the correction factor was neglected. The observed absorption of the 1 mm frog sciatic nerve had a mean value of 3.34%. The approximate absorption correction, considering the nerve as a cylindrical collection of crystallites (International Tables for X-ray Crystallography) is about 1.03 or 3%. Since all five reflections occur within a scattering angle of 1.4°, the absorption correction is likely to be the same for all reflections and no correction for absorption was made. The maximum polarization correction (fifth order reflection) had a value of only 1.001 and was neglected. Based upon published pinhole data (Schmitt et al, 1935) and our own photographs, there was no evidence of overlapping reflections in the region of the first five orders of reflection. A multiplicity of one was assumed. Since the myelin was present in the form of tubes of spiral lamellae, complete interaction would occur for all rays entering the specimen without oscillation or tilting of the specimen.

It was found that all available detail for the first five orders in the diffraction pattern could be obtained with the arrangement (*b*) (Table I). Arrangement (*e*) was used in measuring the large order reflections. The entrance slit width and exit slit width were proven experimentally to be sufficiently narrow so that no slit width collimation error with smearing was introduced. This was shown by successive experiments, in which the entrance slit and exit slit widths were each varied.

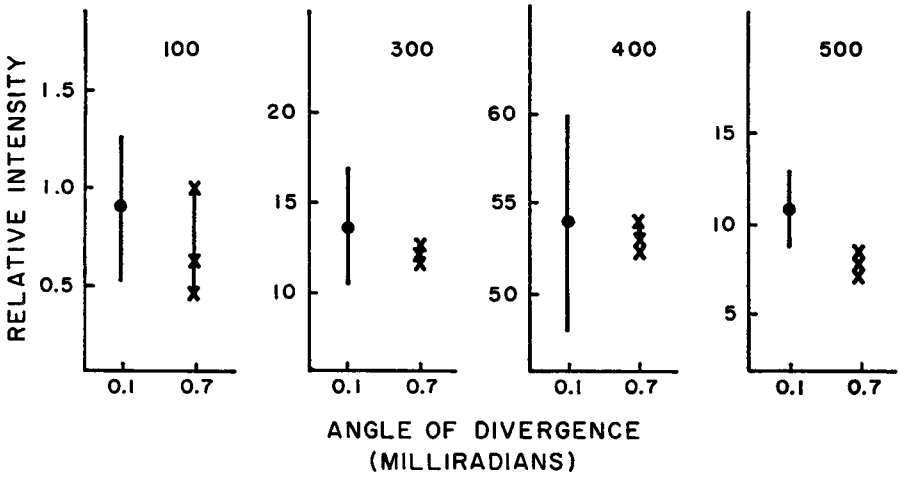

FIGURE 8 The effect of increasing the beam divergence by elevating the collimating bridge with aluminum foil. Normal arrangement of Kratky collimator 0.10 milliradians angle of divergence (16 experiments). Modified Kratky collimator, 0.7 milliradians. Individual data points are shown by ×'s, while at 0.1 milliradians divergence the standard deviation from the mean is shown. The intensities of reflections are relative to the (200) peak which is given a value of 100.0.

The height of the exit slit was large enough so that even though equatorial reflections were arced (as shown by the circular beam pattern), all of the diffracted intensity was collected by the proportional detector. Therefore, no slit height correction (Kratky, Porod, and Skala, 1960) for the arcing of the reflections were made.

The possible effect of disorder of the myelin in the sciatic nerve trunks in the observed intensity distribution was examined by measuring the half-width at half-height of each of the five main reflections. Within the experimental error all reflections (200, 300, 400, 500) had the same peak width at half-height. The average width at half-height was 0.22 ± 0.02 milliradians.

The results of increasing the beam divergence on the measured integrated intensities (relative to the 200 peak intensity) are shown in Fig. 8. With the possible exception of the weak fifth order reflection, the integrated intensities obtained with a $\times 7$ increase in beam divergence agree with those obtained with the normal collimation arrangement. Therefore, beam divergence is not expected to alter the relative integrated intensities of the diffraction peaks which was confirmed experimentally.

DISCUSSION

Relation of Intensity Distribution to Disorder of the Myelin

The question of whether the spectra which have been recorded as consisting of only five major reflections and three weak larger order reflections is limited by disorder or the electron density distribution itself, is the most basic one in attempting to determine the electron density distribution of the myelin membrane. Both the circular beam and the rectangular beam patterns were essentially the same for nerves placed under tensions from 0–40 g (break point for the nerve). There was no increase in intensity of the first five orders. This suggests that the higher order X-ray spectra are not attenuated by disorder due to rippling of the nerve axon along the length of the nerve. Longitudinal rippling of the myelin tubes might occur as a result of elastic shrinkage of a normal taut nerve on removal from the tissues. However, on stretching the nerve with 40 g weight we observed no significant change in the intensity profiles of the reflections whether viewed perpendicular to the nerve by the rectangular beam scan or viewed parallel to the nerve on circular beam photographs. The arcing of the reflections seen in the circular beam photographs must be due to deviations of the myelin bundles from the axis of the nerve. Stretching did not affect the arcing, possibly because the nerve is constrained by the collagen fibers within it. The camera exit slit arrangement is such that the proportional counter sees the entire arc. Therefore, the intensity is not attenuated due to the reflection smearing itself out into the arc.

The light microscope photographs (Fig. 5) indicate a considerable irregularity, or variation in the radius of curvature, of the cross-sectional profiles which might be expected to cause significant damping of the X-ray spectra. However, the average measured half-widths, measured at half-height, are essentially the same within experimental error for the (200), (300), (400), and (500) reflections.

The observed breadth at half-height of each of the first five strong reflections is 0.22 ± 0.02 milliradians. The myelin sheath consists of approximately 75 layers of a 171 A double membrane repeat unit. A peak width at half-height of 0.23 milliradians (Klug and Alexander, 1962) was calculated for this number of repeat units. A significant amount of disorder would have caused the observed half-width to be greater than the calculated one, and also the half-widths would have increased in the higher orders of the reflections. If there is disorder in the packing of the membrane in the myelin sheath, then the effect is less than the experimental error in measurement.

Therefore, the apparent attenuation of the intensity spectra is not due to disorder of the membrane within the myelin sheath. We conclude that the absence of strong reflections beyond the fifth order is a consequence of the nature of the membrane radial electron density distribution itself.

Interpretation of the Data

Phase angles of the X-ray diffraction reflections and the calculated electron density distribution are discussed in the following paper (part II). Our conclusion that the number of major reflections (five) is not limited by disorder of the membrane, but is a result of the particular electron density distribution across the myelin membrane pair, is unexpected on the basis of the bilayer model of the membrane (Davson and Danielli, 1943; Vandenheuvel, 1963). The crystalline or semicrystalline inner layer of hydrocarbon chains and cholesterol postulated by these models should result in a step-function type of electron density distribution. The protein layer would be the highest step with the hydrocarbon tails of the lipid forming a low level step in the center of the electron density distribution of the membrane. The Fourier transform of a step function was calculated. An inverse transform was then taken using an increasing number of terms to see how many terms were needed to define the step function. The step function started to take shape when six terms were used, and was only well defined when eighteen terms were used. Therefore, to describe the diffraction pattern of a step function does require many more orders of reflections (Fourier transform terms) of significant intensity than are actually observed (Bracewell, 1965). Past workers (Finean and Burge, 1963; Worthington and Blaurock, 1968) have tried to fit a step-function electron density to their electron density map assuming that disorder within the nerve bundle caused the larger orders to become nonobservable. The pinhole diffraction pattern as well as the slit beam diffraction patterns do not justify such an assumption. Therefore, the limitation of five major reflections and three very weak high order reflections indicate that the electron density distribution is a modified cosine function (with added detail determined by the 6th, 8th, and 11th orders). We conclude that the membrane is not made up of sharply distinct lamellae of differing electron density.

The intensity data has been shown to be essentially unmodified either by disorder or experimental conditions. The data can now be used, together with reevaluated

phase data, to calculate the electron density of the membrane. Using the improved phasing techniques described in part II of this report, we intend to explore the electron density distribution calculated from the X-ray diffraction data and its relationship to the interpretation of the membrane structure from electron microscopy.

We thank Dr. A. Guinier, University of Paris, and Dr. W. J. Walbesser, State University of New York at Buffalo, for their advice, Roger Moretz and Ali Hamad for assistance with the electron microscopy.

This work was, in part, supported by National Science Foundation Grant GB-7130, American Cancer Society Grant E-457 and IN54H-6.

Received for publication 25 June 1969 and in revised form 4 August 1969.

REFERENCES

BLASIE, J. K., M. M. DEWEY, A. E. BLAUROCK, and C. R. WORTHINGTON. 1965. *J. Mol. Biol.* **14**:143.

BLAUROCK, A. E., and C. R. WORTHINGTON. 1969. *Biochim. Biophys. Acta.* **173**:419.

BRACEWELL, R. 1965. The Fourier Transform and Its Application. McGraw-Hill Book Company, New York. 156.

BURGE, R. E., and J. C. DRAPER. 1965. *Lab. Invest.* **14**:978.

BURGE, R. E., and J. C. DRAPER. 1967. *J. Mol. Biol.* **28**:173.

DAVSON, H., and J. F. DANIELLI. 1943. The Permeability of Natural Membranes. Cambridge University Press, London.

DULBECCO, R., and M. VOGT. 1954. *J. Exp. Med.* **99**:167.

FERNANDEZ-MORAN, H., and J. B. FINEAN. 1957. *J. Biophys. Biochem. Cytol.* **3**:725.

FINEAN, J. B. 1953. *Exp. Cell Res.* **5**:202.

FINEAN, J. B. 1958. *Exp. Cell Res. Suppl.* **5**:18.

FINEAN, J. B. 1962. *Circulation.* **26**:1151.

FINEAN, J. B. 1965. *Ann. N.Y. Acad. Sci.* **122**:51.

FINEAN, J. B., and R. E. BURGE. 1963. *J. Mol. Biol.* **7**:672.

FINEAN, J. B., R. COLEMAN, W. A. GREEN, and A. R. LIMBRICK. 1966 *a. J. Cell Sci.* **1**:287.

FINEAN, J. B., R. COLEMAN, and W. A. GREEN. 1966 *b. Ann. N.Y. Acad. Sci.* **137**:414.

FINEAN, J. B., F. S. SJOSTRAND, and E. STEINMANN. 1953. *Exp. Cell Res.* **5**:557.

HUSSON, F., and V. LUZZATI. 1963. *Nature (London).* **197**:822.

International Tables for X-Ray Crystallography, Kynoch Press, Birmingham, England, **2**:295.

KLUG, M. P., and L. E. ALEXANDER. 1962. X-ray Diffraction Procedures. John Wiley & Sons, Inc., New York. Chap. 9.

KRATKY, O., G. POROD, and Z. SKALA. 1960. *Acta Phys. Austriaca.* **13**:76.

KRATKY, O. 1963. *Prog. Biophys. Mol. Biol.* **13**:105.

LUFT, J. H. 1961. *J. Biophys. Biochem. Cytol.* **9**:409.

MOODY, M. F. 1963. *Science (Washington).* **142**:1173.

NORTON, W. T., and L. A. AUTILIO. 1965. *Ann. N.Y. Acad. Sci.* **122**:77.

O'BRIEN, J. S. 1967. *J. Theoret. Biol.* **15**:307.

PALADE, G. E. 1952. *J. Exp. Med.* **95**:285.

PEASE, D. C. 1964. Histological Techniques for Electron Microscopy. Academic Press, Inc., New York. 2nd edition. 52.

ROBERTSON, J. D. 1966. *Ann. N.Y. Acad. Sci.* **137**:421.

SCHMITT, R. O., R. S. BEAR, and G. L. CLARK. 1935. *Radiology.* **25**:131.

SILVESTER, N. R. 1964. *J. Mol. Biol.* **8**:11.

VANDENHEUVEL, F. A. 1963. *J. Amer. Oil Chem. Soc.* **40**:455.

VENABLE, J. H., and R. COGGESHALL. 1965. *J. Cell Biol.* **25**:407.

WORTHINGTON, C. R. 1960. *J. Mol. Biol.* **2**:327.

WORTHINGTON, C. R., and A. E. BLAUROCK. 1968. *Nature (London).* **218**:87.